SRNL-STI-2012-00257
Rev. 0

DESTRUCTIVE EXAMINATION OF SHIPPING PACKAGE 9975-03431

W. L. Daugherty

Savannah River National Laboratory
Materials Science & Technology

Publication Date: May 2012

Savannah River Nuclear Solutions
Savannah River Site
Aiken, SC 29808

This document was prepared in conjunction with work accomplished under Contract No. DE-AC09-08SR22470 with the U.S. Department of Energy.

DISCLAIMER

DESTRUCTIVE EXAMINATION OF SHIPPING PACKAGE 9975-03431

APPROVALS:

W. L. Daugherty _____ Date _____
Author, Materials Science and Technology

T. E. Skidmore _____ Date _____
Technical Review, Materials Science and Technology

K. A. Dunn _____ Date _____
Pu Surveillance Program Lead, Materials Science and Technology

G. T. Chandler _____ Date _____
Manager, Materials App & Process Tech

E. R. Hackney _____ Date _____
NMM Engineering

REVIEWS:

D. R. Leduc _____ Date _____
Savannah River Packaging Technology

J. W. McEvoy _____ Date _____
9975 Shipping Package Design Authority

Revision Log

Document No. SRNL-STI-2012-00257 **Rev. No.** 0

Document Title Destructive Examination of Shipping Package 9975-03431

Rev. #	Page #	Description of Revision	Date
0	all	Original document	5/30/2012

Nomenclature

ASTM – American Society for Testing and Materials

DSA – Documented Safety Analysis

FT-IR – Fourier Transform Infrared Spectroscopy

ID – Inside Diameter

KAC – K-Area Complex

OD – Outside Diameter

PCV - Primary Containment Vessel

RH – Relative Humidity

SAT – Satisfactory

SCV – Secondary Containment Vessel

SEM – Scanning Electron Microscope

SPA – Surveillance Program Authority

SRNL – Savannah River National Laboratory

SRS – Savannah River Site

UNSAT – Unsatisfactory

WME – Wood Moisture Equivalent

Destructive Examination of Shipping Package 9975-03431

Summary

Destructive and non-destructive examinations have been performed on specified components of shipping package 9975-03431. For those attributes that were also measured during the field surveillance, no significant changes were observed. All observations and test results met identified criteria, or were collected for information and trending purposes. Except for modest corrosion of the lead shield (which is typical of these packages following several years service), no evidence of a degraded condition was found in this package.

Introduction

The Savannah River Site (SRS) stores packages containing plutonium (Pu) materials in the K-Area Complex (KAC). The Pu materials are packaged per the DOE 3013 Standard and stored within Model 9975 shipping packages in KAC.

The KAC facility DSA (Document Safety Analysis) [1] credits the Model 9975 package to perform several safety functions, including criticality prevention, impact resistance, containment, and fire resistance to ensure the plutonium materials remain in a safe configuration during normal and accident conditions. The Model 9975 package is expected to perform its safety function for at least 12 years from initial packaging. The DSA recognizes the degradation potential for the materials of package construction over time in the KAC storage environment and requires an assessment of materials performance to validate the assumptions of the analysis and ultimately predict service life.

As part of the comprehensive Model 9975 package surveillance program [2-3], destructive examination of package 9975-03431 was performed following field surveillance in accordance with Reference [4]. Field surveillance of the Model 9975 package in KAC included nondestructive examination of the drum, fiberboard, lead shield and containment vessels [5]. Results of the field surveillance are provided in Attachment 1.

Package History

Fabrication of package 9975-03431 was completed by Joseph Oat Corporation on June 24, 2004 and shipped to the Savannah River Site. Annual maintenance was performed on the package by SRNL on November 28, 2007. After transfer to Lawrence Livermore National Laboratory (LLNL), it was loaded with plutonium oxide material packaged in accordance with DOE-STD-3013 on January 31, 2008. The contents generated approximately 10 watts heat load. LLNL shipped this package to KAC, where it was received on February 21, 2008. Routine field surveillance was performed on January 5, 2012. SRNL received the package on February 22, 2012 and performed destructive examination activities between February 23 and April 18, 2012. (The history of this package between July 2004 and November 2007 has not been identified.)

Discussion

The results of the field surveillance [6] were reviewed. No unsatisfactory conditions were noted. As the package was opened, and components removed, each component was marked to identify its orientation within the package. For components that were removed during the field surveillance, their orientation at the time of this examination probably bears no relation to their orientation while stored in KAC. However, the bottom fiberboard subassembly and lead shield would likely have remained in the same orientation they occupied in KAC.

Examination activities are documented through photographs, data sheets, and other documents. This documentation is maintained in a laboratory notebook [7]. The following examination activities were performed:

Fiberboard physical properties:

The weight and dimensions of the top and bottom fiberboard subassemblies were measured. The weight of the top subassembly was 12.865 kg (28.36 lb). During the field surveillance, the measured weight of the top subassembly was 28.3 lb. These two values are in good agreement. Weight and dimension data are recorded in Table 1.

The air shield was cut and peeled back at four locations to permit accurate measurement of the top fiberboard subassembly dimensions. In order to calculate the density of each subassembly, nominal dimensions were assumed for the aluminum bearing plate and air shield. The calculated densities (0.290 g/cc top subassembly, 0.296 g/cc bottom subassembly) meet the limit for the criticality control function, 0.20 g/cc minimum [4]. The volume and density were calculated using the following equations (see the Table 1 sketch for dimension nomenclature).

Top subassembly fiberboard volume,

$$V_U = (UD1)^2 (UH1) (\pi/4) + [(UD1) - 2 (UR2)]^2 (UH2) (\pi/4) - (UD2)^2 (UH3) (\pi/4) - 59.96 \text{ inch}^3$$

Top subassembly fiberboard weight, W_U = upper subassembly weight – 9.773 lb

Top subassembly fiberboard density, $\rho_U = W_U / V_U$

Bottom subassembly fiberboard volume,

$$V_L = (LD1)^2 (LH1) (\pi/4) - [(LD2) + 2 (LR1)]^2 (LH3) (\pi/4) - (LD2)^2 (LH2) (\pi/4) - 59.96 \text{ inch}^3$$

Bottom subassembly fiberboard weight, W_L = bottom subassembly weight – 4.827 lb

Bottom subassembly fiberboard density, $\rho_L = W_L / V_L$

Fiberboard dimensions measured during field surveillance are summarized in Attachment 1, and are consistent with drawing requirements and destructive examination measurements. For each of the five dimensions measured in both the field surveillance and destructive examination, the measured values are similar. The dimensions were measured twice during destructive examination, 49 and 75 days after the field surveillance. Although the changes in measured fiberboard dimensions vary, they are generally in a consistent direction from field surveillance through the two destructive examination measurements. This would suggest that the

dimensional variation results primarily from the continuing redistribution of moisture within the fiberboard. No significant observations were found with the fiberboard physical measurements.

Fiberboard visual appearance:

No significant material or physical damage was observed, and layers were well bonded. The lower subassembly was snug within the drum, but came out smoothly without interference. Following removal of both the top and bottom fiberboard subassemblies from the outer drum, both were inspected visually. No anomalous conditions were observed.

Fiberboard moisture content:

The moisture content of the fiberboard will affect its properties, including density, mechanical strength and thermal properties. Measuring the moisture content of the top and bottom subassemblies, and the relative humidity inside the package, provides reference data to potentially correlate laboratory test results with behavior in KAC. The fiberboard moisture content was measured twice during destructive examination activities – upon receipt of the package, and again approximately 4 weeks later. Measurements were also taken during field surveillance to the extent the fiberboard was accessible.

A GE Protimeter Surveymaster moisture probe was used to measure the moisture content of the top and bottom fiberboard subassemblies. This probe identifies the wood moisture equivalent (WME), or the weight % of moisture that would produce the same electrical conductivity in wood. Moisture content data are presented in Figure 1.

Moisture measurements were compared to those taken during previous destructive examinations [8 – 13]. The readings on 9975-03431 are lower on average than seen on previous packages. During field surveillance, the measured moisture content of accessible regions of the fiberboard ranged from 6 to 10 %WME. During subsequent examination, with both upper and lower fiberboard assemblies removed, moisture content ranged from 6.5 to 12.6 %WME.

A moisture gradient of 3.5 %WME was observed across the upper fiberboard assembly side wall during field surveillance. During the subsequent inspections, this gradient decreased to 1.5 %WME. The moisture gradient across the lower assembly side wall was not recorded during field surveillance, but was 3.4 %WME 35 days later, and 3.1 %WME 61 days later. This is consistent with other packages examined – the larger moisture gradient tends to develop in the lower assembly, and the gradient in both assemblies decreases gradually after the internal heat load is removed.

Consistent with recent efforts to correlate moisture content of fiberboard with humidity in the surrounding air, data were taken to correlate these two parameters. The fiberboard was placed back in the drum with a narrow channel cut down the side. A humidity probe was placed in this channel such that it could be raised and lowered with the drum closed. The edge of the drum lid was taped to seal around the gap created by the humidity probe cable. After humidity levels in the drum reached equilibrium, humidity readings were taken at several elevations along the fiberboard, and the fiberboard was then removed to measure the moisture content at those same

locations. This process was repeated to demonstrate consistency in the results. These data are summarized in Figure 2, and compared to similar data from two previous packages and laboratory samples. All the data show a similar trend, although the data for the 9975 packages are offset slightly from that for laboratory samples.

Fiberboard thermal and mechanical properties:

Samples of fiberboard were removed from the bottom fiberboard subassembly to measure compressive strength, specific heat capacity and thermal conductivity. The source location(s) of these samples is illustrated in Figures 3 and 4. The thermal conductivity sample from the bottom center of the subassembly is oriented for heat flow in the axial direction (perpendicular to the glue joints). The thermal conductivity sample from the side is oriented for heat flow in the radial direction (parallel to the glue joints). Testing on each sample was performed at a nominal (mean) temperature of approximately 25ºC (77ºF), with no environmental conditioning. Physical data on the fiberboard samples are recorded in Table 2.

The compression test data are shown in Figures 5 and 6, along with select baseline data. For both the perpendicular and parallel orientations, the compression strength of the 9975-03431 samples is similar to the baseline samples conditioned at 77ºF and 70% RH. A series of photographs showing typical compression behavior under parallel loading is shown in Figure 7. The area under the stress-strain curve up to 40% strain is used as a relative indication of the energy absorption capacity of the fiberboard. This metric is shown in Figure 8 for each destructively examined package as a function of fiberboard moisture content. In general, the energy absorption capacity decreases as the moisture content increases. The results from 9975-03431 are circled in Figure 8. The Figure 8 data collectively show a trend consistent with undegraded fiberboard.

A total of six samples were prepared from the side and base of the lower subassembly for measuring the specific heat capacity of the fiberboard. The specific heat capacity was calculated in accordance with ASTM C351 at a mean temperature of ~25ºC (77ºF). This ASTM Standard specifies test temperatures that would produce a mean test temperature of 60ºC, but allows alternate test temperatures to be substituted as needed. Data were collected for a sample target temperature of 45ºC, and a water temperature of ~5ºC. The sample moisture content was 7.9 – 9.6 % WME (wood moisture equivalent). Each sample was tested four times, and all results were averaged. The average specific heat capacity value was 910 J/kg-K. Multiplying this value by the density of the lower subassembly (296 kg/m^3) gives a heat capacity of 256,000 J/m^3-K (3.82 Btu/ft^3-F). This meets the required minimum value of 3 Btu/ft^3-F. The specific heat capacity value is lower than typical baseline laboratory data, and is lower than observed in previous destructive examination packages. The relatively low moisture content of this package only partially explains this difference.

The thermal conductivity of the fiberboard was measured with a Lasercomp Inc. Fox 300 thermal conductivity instrument at a mean temperature of 25ºC (77ºF). For the sample with axial heat flow (perpendicular to the fiberboard layers), the measured thermal conductivity is 0.0623 W/m-K (0.0360 Btu/hr-ft-ºF). For the sample with radial heat flow (parallel to the fiberboard layers), the measured thermal conductivity is 0.1040 W/m-K (0.0601 Btu/hr-ft-ºF). Both thermal

conductivity values fall within the identified range [4], and are consistent with typical baseline laboratory data [14].

Lead shield visual examination:

The entire surface of the lead shield was visually examined. It was found to be free from significant deformation and physical damage, but the outside surface (in contact with the fiberboard) was covered with a light to moderate layer of white corrosion product (Figure 9). No flaking or blistering of the corrosion product was observed. From prior examination of the shield from package 9975-02234, the corrosion product was identified as basic lead carbonate (hydrocerrusite), $Pb_3(CO_3)_2(OH)_2$ [8]. No further characterizations of the corrosion product were performed.

Lead Shield Dimensions:

Several lead shield dimensions were measured (Table 3) and all are consistent with drawing requirements.

The radial thickness was measured near the top of the shield, and was calculated from diametral data taken near the bottom of the shield. The calculated thickness from near the bottom (0.547 inch) is essentially the same as the measured thickness near the top (0.553 inch). While lead is known to creep at ambient temperatures, these data suggest that no significant creep deformation has occurred thus far, since creep would tend to reduce the thickness near the top relative to the bottom.

O-ring examination and testing:

Prior surveillance testing of the four O-rings from this package included visual examination, dimensional and hardness measurements. Dimensional measurements were repeated on each O-ring as part of the destructive examination. Three of these O-rings (SCV outer, PCV outer and PCV inner) received additional testing. All three were submitted for FT-IR spectroscopy to confirm material composition, and the two outer O-rings received optical and SEM microscopic examination of the cross section. The dimensions and weight of the SCV outer and PCV outer O-rings were recorded to calculate their density. The PCV inner O-ring was tensile tested, including a hold point at 50% strain to visually examine the O-ring.

Weight and dimension data for the two outer O-rings are presented in Table 4. The average minor diameter for each O-ring is within the specified tolerances for new O-rings, but the major inside diameter for each O-ring (calculated from the length measured after the O-ring was cut) is greater than specified for new O-rings. This is consistent with a permanent stretch due to the lid diameter. Leak testing during the field surveillance was successful.

Compression set was calculated for each O-ring based on each of the dimensional measurements it received. Compression set is calculated as follows, assuming an initial minor diameter of 0.139 inch and an average groove depth in the lid of 0.0995 inch.

Compression set (%) = (0.139 - radial thickness) / (0.139 - 0.0995)*100

These values are shown in Figure 10 as a function of time since removal of the O-rings, for the current package as well as for 9975-02168 for comparison. The compression set decreases with time, as the polymer continues to relax. For 9975-03431 O-rings, the compression set levels off after 50 – 60 days, while this occurs around 20 – 30 days for 9975-02168 O-rings.

FT-IR spectroscopy generically identified the composition of each O-ring as consistent with a Viton® type fluoroelastomer (Figure 11). Viton® A produces a spectrum nearly identical to Viton® GLT, the base polymer for the specified O-ring compound (Parker Seals V0835-75) and the two are difficult to distinguish by FT-IR analysis alone. Additional test techniques (e.g. dynamic mechanical analysis, DMA) would be required to uniquely verify the GLT composition. These results are similar to those from previous destructive examination packages [8 – 13] and are consistent with baseline data [15].

As with previous destructive examinations, visual (Figure 12) and SEM (Figure 13) examination of the cross sections identified a distribution of very small particles throughout each O-ring. Aside from carbon and fluorine (which are the primary constituents of Viton®) the SEM identified the presence of aluminum, silicon, oxygen and zinc. These elements are present in small amounts, and are generally associated with the particles. Though the actual compound is proprietary, zinc and oxygen are consistent with Viton®-type fluoroelastomer compounds, which typically contain MgO, CaO, $Ca(OH)_2$, ZnO or lead compounds as acid acceptors and heat stabilizers [16]. Aluminum is present in hydrotalcite, which is used in both GLT and GLT-S compounds as a filler reinforcing agent. Silicon may be present as a trace contaminant.

The PCV inner O-ring was tensile tested in accordance with ASTM D1414, using a cut (single strand) sample. The test was interrupted at 50% strain (Figure 14) to visually examine the O-ring for signs of cracking or other degradation. None were observed. The stress-strain curve for the PCV inner O-ring is shown in Figure 15 along with curves from a new O-ring and from previous destructive examinations. The O-ring from package 9975-03431 displayed tensile properties (strength and elongation) consistent with that observed in previous examinations. The elongation (290%) of this O-ring exceeds the minimum value specified in AMS-R-83485 for new O-rings (120%), while the tensile strength (1.6 ksi) matches the minimum value specified (1.6 ksi) [15]. While Parker Seals does not change the formulation of these O-rings, there are batch variations.

General:

A general visual examination was performed on all metallic components. Aside from the corrosion of the lead shield (discussed above) no significant damage or degradation was observed. Several components were observed to have fabrication markings. Various markings were stamped or engraved on the containment vessels and lids. These markings appear to be identification numbers used during manufacture, prior to association of the parts with a final package number, and are consistent with those seen in other packages.

The distance from the drum flange to the top of the air shield was measured, and ranged from 0.780 to 0.862 inch. The average value was 0.820 inch. During the second examination at SRNL, the average air gap was found to have decreased to 0.798 inch. The drum drawing [17] identifies a reference value for this dimension as 0.8 inch, and notes that it may vary over time due to variations in fiberboard properties. Pre-operational verification requirements, consistent with fire and drop test qualifications for the 9975 package, specify this dimension be no greater than 1 inch. During field surveillance, the average value of this dimension was 0.722 inch. The increase in this dimension likely resulted during transport of the package to SRNL - the dynamic conditions of transport may have caused some compaction of the fiberboard.

The data from the examination activities described above are compared with field surveillance data in Attachment 1. All specified criteria were met during this examination. All observations and examination results are consistent with expectations. All findings will be reviewed by NMM for potential impact on the continued storage of other packages in KAC.

Measurement Uncertainties:

Numerous measurements were made with a variety of instruments during the destructive examination of package 9975-03431. Some of the measurements were specifically compared to inspection criteria, while others were taken for information / trending purposes. All measurements which are compared to inspection criteria were made with calibrated instruments, or were verified against calibrated instruments. The uncertainties associated with measurements and calculated results required to meet inspection criteria are discussed below.

Weight – The weight of each fiberboard subassembly was measured to a precision of 1 gram. The balance used was M&TE, and the calibration data show an accuracy within 5 grams over the range of interest. A conservative net uncertainty of 6 grams will be used.

Calipers – Three different calipers were used to measure component dimensions. All three calipers are M&TE, and calibration data show an accuracy within 0.001 inch. In addition, operator bias can affect measurement accuracy through the contact load applied when making a measurement. A degree of give exhibited by the fiberboard will lead to different results as the contact load changes. The larger calipers are judged to be more susceptible to this bias. Metallic components are significantly more rigid than the fiberboard, but operator bias may also exist for those components. While not characterized explicitly, it is judged that the total uncertainty (instrument uncertainty plus operator bias) for fiberboard measurements is no greater than +/- 0.003 inch for the 6 inch calipers, +/- 0.005 inch for the 24 inch calipers, and +/- 0.007 inch for the 40 inch calipers. It is further judged that total uncertainty when measuring metallic components is no greater than +/- 0.003 inch for 6 and 24 inch calipers, and +/- 0.005 inch for the 40 inch calipers.

Manual calipers – Dimension ID2 on the lead shield was captured with manual swing calipers, which was then locked in that position and measured with 24-inch calipers. It is judged that the accuracy of capturing this dimension with the manual calipers is within +/- 0.002 inch, and the measurement of that dimension is then within +/- 0.002 inch, for a (conservatively) combined accuracy of +/- 0.004 inch.

Thermal conductivity instrument – The specifications for the Fox300 thermal conductivity instrument include a stated accuracy of ~1%. Measurement of the thermal conductivity of a calibration standard was accurate to within 1.1%. Prior test reports of fiberboard samples from an independent laboratory, using the same model instrument, identified an overall 3% uncertainty. An uncertainty of 3% will be conservatively assumed for the current measurements.

Heat capacity – The specific heat capacity is derived from temperature and weight measurements, using calibrated instruments. The thermocouple and balance precisions are high. The greatest contribution to error in the specific heat capacity is considered to be consistency of operator technique. The total uncertainty is reflected in the range of results for multiple trials. The heat capacity was measured four times on each of six samples. The variation for each sample ranged from 7 to 52%. The combined uncertainty on the average of 6 samples is 14%.

Where measurement results are used in subsequent calculations, the uncertainty values identified above are assumed to be random. A standard error propagation formula for random errors is used to calculate the final result uncertainty. In some cases, the calculated uncertainty may be less than the potential error from rounding off the result, and the higher variation associated with round-off is reported as the uncertainty. These calculations are documented in the Laboratory Notebook [7]. Calculation results and their uncertainties are summarized as follows:

- Top fiberboard subassembly volume = 29028 +/- 26 cm^3
- Top fiberboard subassembly density = 0.290 +/- 0.001 g/ cm^3
- Bottom fiberboard subassembly volume = 85934 +/- 73 cm^3
- Bottom fiberboard subassembly density = 0.296 +/- 0.001 g/ cm^3
- Shield radial thickness at bottom = 0.547 +/- 0.003 inch
- Thermal conductivity (radial) = 0.0601 +/- 0.002 Btu/hr-ft-ºF
- Thermal conductivity (axial) = 0.0360 +/- 0.001 Btu/hr-ft-ºF
- Heat capacity = 3.8 +/- 0.5 Btu/ft^3-ºF

References

[1] WSRC-SA-2002-00005, Rev. 1CN-7, “K-Area Material Storage Facility Documented Safety Analysis”, June 2008.

[2] SFS-ENG-99-0085, “Summary and Guide to 9975 Container Qualification Program”

[3] WSRC-TR-2001-0286, Rev. 4, “The Savannah River Site Surveillance Program for the Storage of 9975/3013 Plutonium Packages in KAC”, July 2008

[4] WSRC-TR-2005-00135 Rev. 1, “Task Technical and Quality Assurance Plan for Destructive Examination of a 9975 Package from Field Surveillance Activities”, W. L. Daugherty, March 2011

[5] WSRC-TR-2004-00197, "Inspection Activities and Acceptance Criteria for Field Surveillance of Model 9975 Package O-Rings and Celotex® Materials", W. L. Daugherty, April 2004

[6] SOP-CSS-207-K, Rev. 8, Attachment 2 "9975 Surveillance Data Sheet" for surveillance SRNS-SRV-2011-009

[7] WSRC-NB-2008-00002, Laboratory Notebook "9975 Shipping Package Celotex Testing Book III, and SRNL-NB-2012-00048, Laboratory Notebook "9975 Shipping Package Celotex Testing Book IV

[8] WSRC-TR-2005-00273, Rev. 1, "Destructive Examination of Shipping Package 9975-02234", W. L. Daugherty, September 2005

[9] WSRC-TR-2006-00162, "Destructive Examination of Shipping Package 9975-00826", W. L. Daugherty, May 2006

[10] WSRC-STI-2007-00558, "Destructive Examination of Shipping Package 9975-00600", W. L. Daugherty, October 2007

[11] SRNS-STI-2008-00019, "Destructive Examination of Shipping Package 9975-05128", W. L. Daugherty, August 2008

[12] SRNL-STI-2009-00763, "Destructive Examination of Shipping Package 9975-02028", W. L. Daugherty and T. M. Stefek, December 2009

[13] SRNL-STI-2010-00654, "Destructive Examination of Shipping Package 9975-02168", W. L. Daugherty, November 2010

[14] SRNL-MST-2008-00038, "Properties of Un-Aged Cane Fiberboard for Thermal Modeling", W. L. Daugherty, February 22, 2008

[15] WSRC-TR-2004-00162, "Baseline Characterization of Model 9975 Shipping Package O-Rings", T. E. Skidmore, March 2004

[16] Rubber Technology Handbook, W. Hofmann, Hanser Publishers, New York, 1989, page 122

[17] Drawing R-R2-F-0025, Rev. 5, "9975 Drum with Flange Closure Subassembly & Details"

Table 1. Fiberboard physical measurements and calculated density

Top Subassembly						
Weight	12.865 kg					R-R2-F-0019 Rev 5
	0/180 deg.		90/270 deg.		Avg.	Nominal value (inch)
UD1 (in)	17.696		17.672		17.684	17.7
UD2 (in)	8.552		8.545		8.548	8.55
	0 deg.	90 deg.	180 deg.	270 deg.	Avg.	
UR1 (in)	3.048	3.052	3.050	3.055	3.051	3.075
UR2 (in)	1.510	1.486	1.531	1.533	1.515	1.5
UH1 (in)	7.154	7.204	7.175	7.148	7.170	7.1
UH2 (in)	2.137	2.127	2.128	2.126	2.130	2.1
UH3 (in)	5.030	5.044	5.027	5.036	5.034	5.0

Top subassembly calculated density = 0.290 g/cc

Bottom Subassembly						
Weight	27.587 kg					R-R2-F-0019 Rev 5
	0/180 deg.		90/270 deg.		Avg.	Nominal value (inch)
LD1 (in)	18.053		18.056		18.054	18.1
LD2 (in)	8.505		8.514		8.510	8.45
	0 deg.	90 deg.	180 deg.	270 deg.	Avg.	
LR1 (in)	3.261	3.230	3.231	3.256	3.247	3.275
LR2 (in)	1.497	1.495	1.501	1.502	1.499	1.55
LH1 (in)	26.698	26.672	26.690	26.707	26.692	26.7
LH2 (in)	20.479	20.481	20.465	20.473	20.474	20.4
LH3 (in)	2.066	2.054	2.069	2.060	2.062	2.0

Bottom subassembly calculated density = 0.296 g/cc

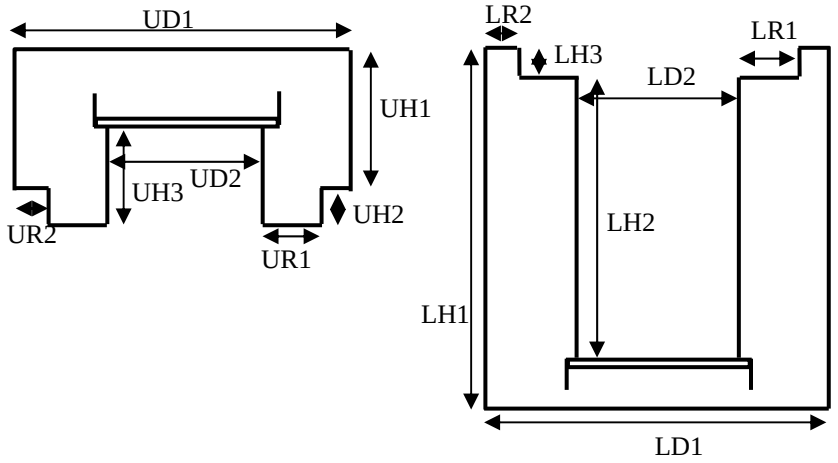

Table 2. Physical data for fiberboard test specimens

Test Sample	Moisture Content (%WME)	Weight (g)	Length (inch)	Width (inch)	Height (inch)	Density (g/cc)
Compression Test Samples						
Side 1 (parallel)	8.5	37.600	2.023	2.039	2.021	0.275
Side 2 (parallel)	8.6	39.507	2.037	2.030	2.017	0.289
Side 3 (perpendicular)	8.2	39.146	2.017	2.040	2.027	0.286
Side 4 (perpendicular)	8.3	39.120	2.041	2.017	2.029	0.286
Base 1 (parallel)	10.1	37.989	2.027	2.000	2.016	0.284
Base 2 (parallel)	9.9	38.444	2.005	2.039	2.018	0.284
Base 3 (perpendicular)	9.6	38.496	2.039	2.015	2.015	0.284
Base 4 (perpendicular)	9.8	38.053	2.007	2.016	2.009	0.286
Thermal Conductivity Samples						
Side (radial)	9.0	296	7.029	6.272	1.467	0.279
Base (axial)	10.5	356	7.008	7.004	1.525	0.290

Table 3. Lead shield dimensions

Dimension	0/180 deg. (inch)		90/270 deg. (inch)		Avg. (inch)	Requirement (inch)
OD (in)	8.324		8.334		8.329	8.252 – 8.35
ID1 (in)	7.236		7.270		7.253	7.25 – 7.26
ID2 (in)	7.265		7.205		7.235	7.24 – 7.26
	0 deg.	90 deg.	180 deg.	270 deg.		
R (in)	0.553	0.555	0.563	0.540	0.553	0.506 min
H (in)	24.634	24.638	24.672	24.656	24.650	24.556 – 24.7

(OD – ID2) / 2 = 0.547 inch

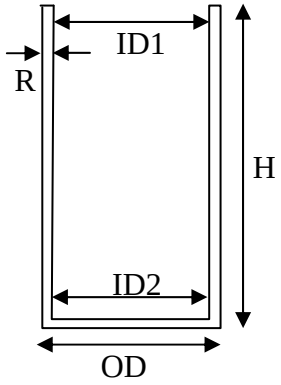

Table 4. O-ring physical data

~60 Days after Field Surveillance	PCV Outer O-Ring Thickness		SCV Outer O-Ring Thickness	
	Radial (inch)	Axial (inch)	Radial (inch)	Axial (inch)
Minor Dia. 0 deg	0.1350	0.1360	0.1400	0.1325
Minor Dia. 45 deg	0.1335	0.1360	0.1380	0.1320
Minor Dia. 90 deg	0.1335	0.1360	0.1375	0.1330
Minor Dia. 135 deg	0.1340	0.1360	0.1395	0.1325
Minor Dia. 180 deg	0.1335	0.1360	0.1405	0.1350
Minor Dia. 225 deg	0.1345	0.1370	0.1405	0.1350
Minor Dia. 270 deg	0.1350	0.1370	0.1405	0.1325
Minor Dia. 315 deg	0.1360	0.1375	0.1405	0.1325
Avg. Minor Dia.	**0.1354 inch**		**0.1364 inch**	
Minor Dia. (new)	0.138 +/- 0.006 inch		0.138 +/- 0.006 inch	
Length (after cut)	14 0/32 inch		17 7/32 inch	
Calculated Major Dia.	4.456 inch avg		5.481 inch avg.	
Major Inside Dia. (new)	4.234 +/- 0.030 inch		5.234 +/- 0.035 inch	
Weight	5.963 g		7.246 g	
Calculated Volume	0.2016 $inch^3$ (3.304 cm^3)		0.2516 $inch^3$ (4.123 cm^3)	
Calculated Density	**1.80 g/cm^3**		**1.76 g/cm^3**	

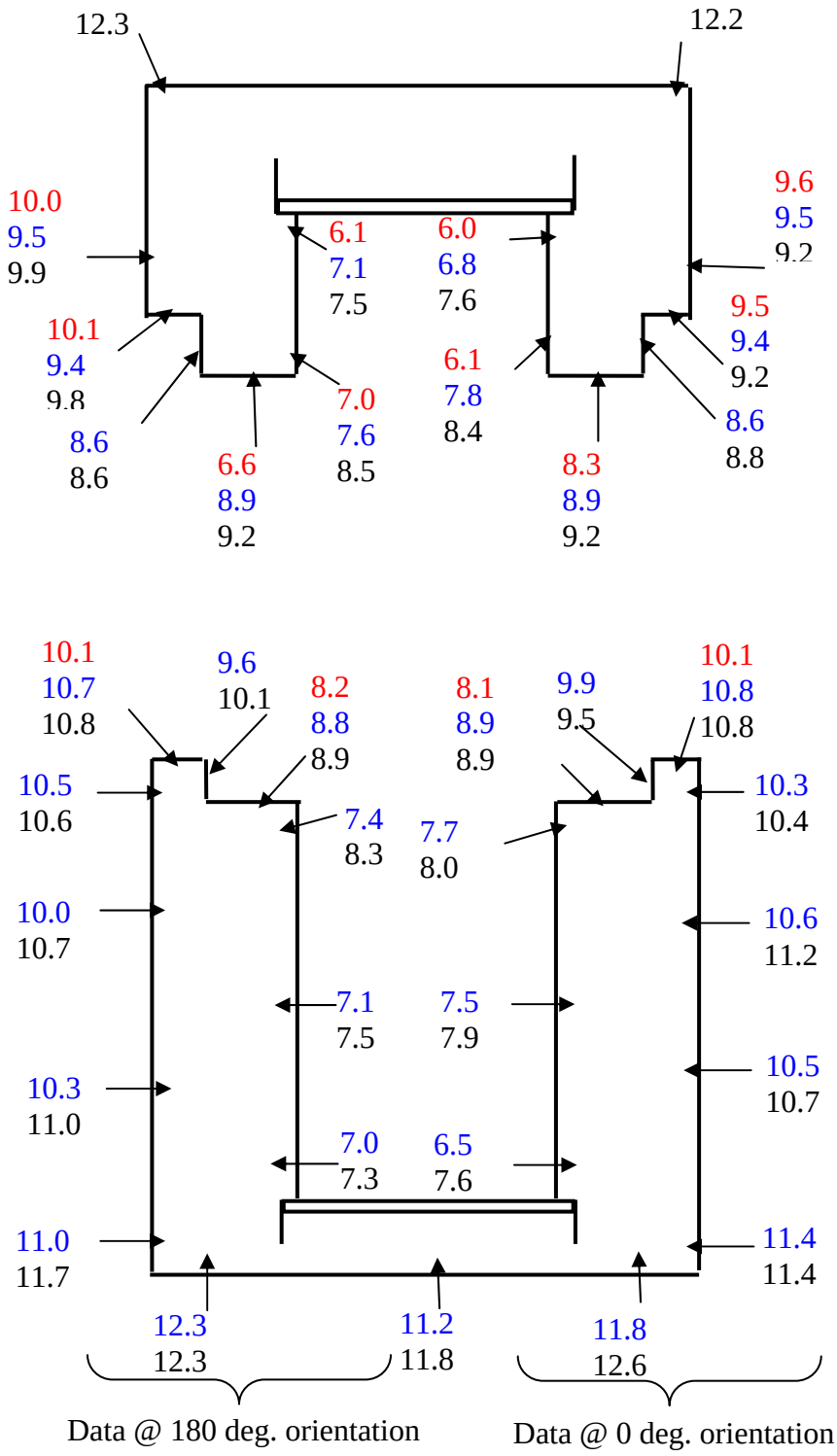

Figure 1. Fiberboard moisture content data. The values in red were measured during field surveillance. The values in blue were measured 35 days later, while the values in black were measured 61 days after field surveillance. All values are % wood moisture equivalent.

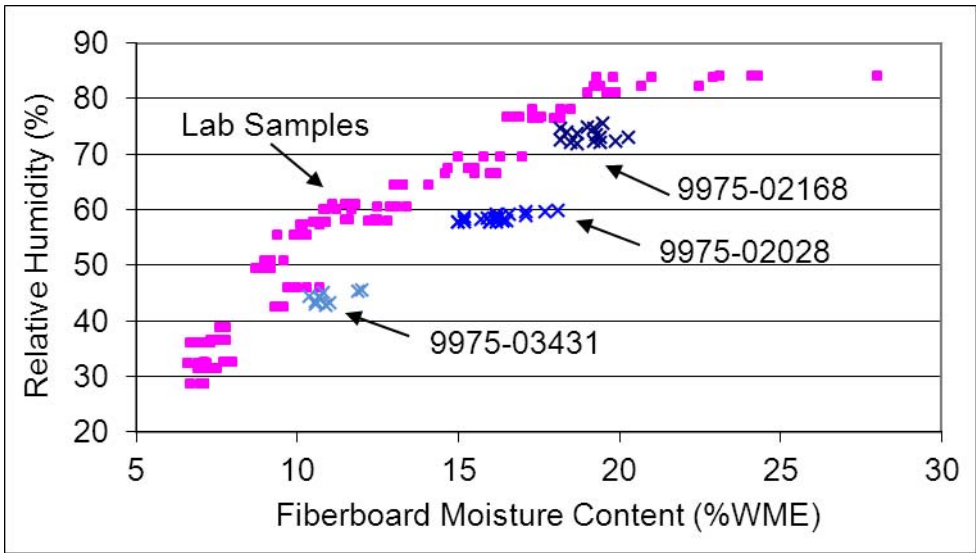

Figure 2. Correlation between fiberboard moisture content and relative humidity of the adjacent air. Data from 9975-03431 are shown with comparable data from 9975-02028, 9975-02168 and laboratory samples. Measurements were taken along the fiberboard OD surface.

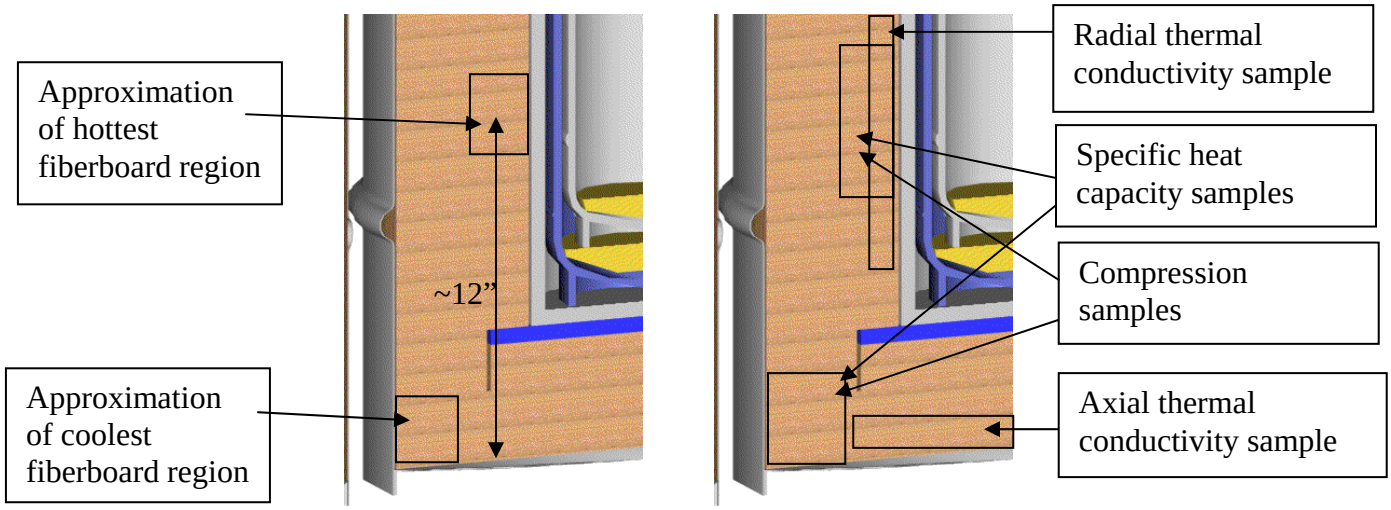

Figure 3. Illustration of fiberboard regions of the bottom subassembly to be tested. Multiple samples (where used) were removed from the illustrated locations at different circumferential positions. Not to scale.

Figure 4. Lower fiberboard assembly (upside down) marked for removal of test samples

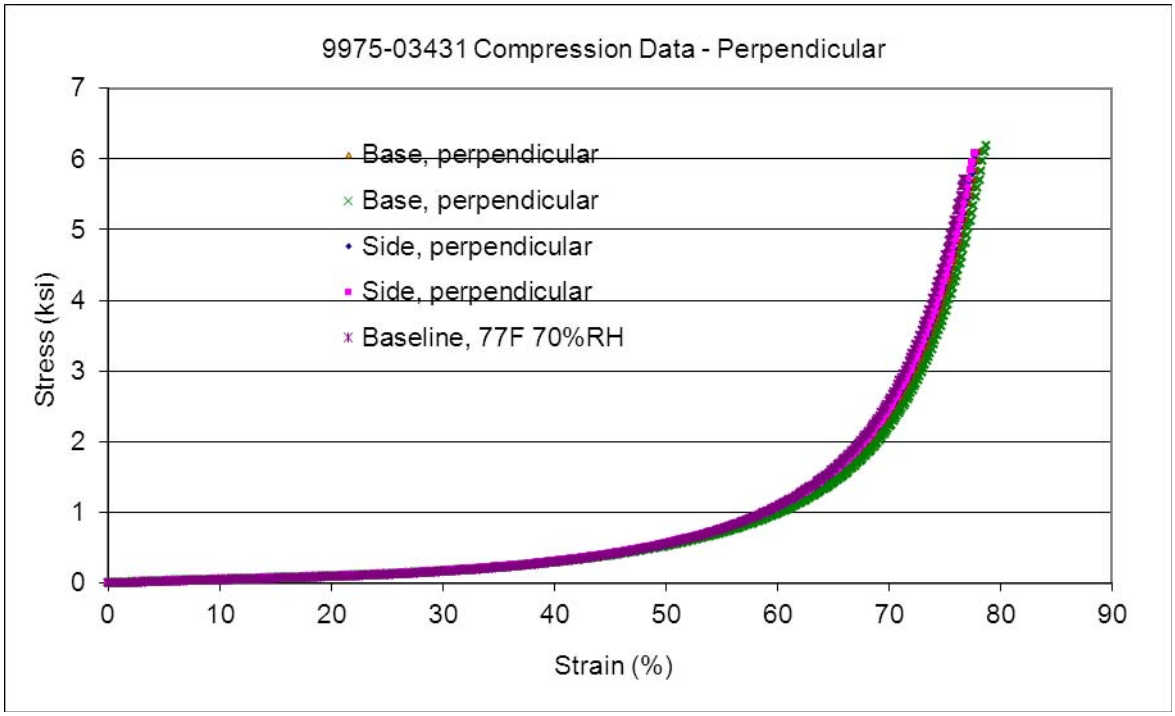

Figure 5. Fiberboard compression test data, compared with typical baseline (77°F, 70% RH) data, in the perpendicular orientation (i.e. load applied perpendicular to the fiberboard layers).

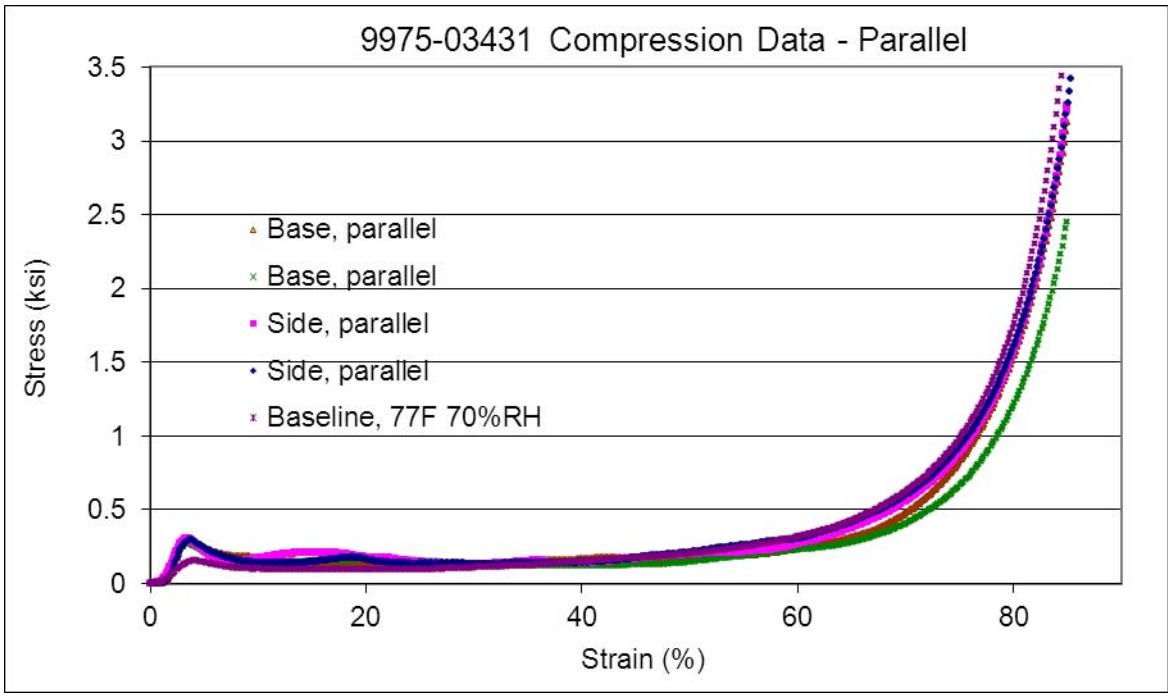

(a)

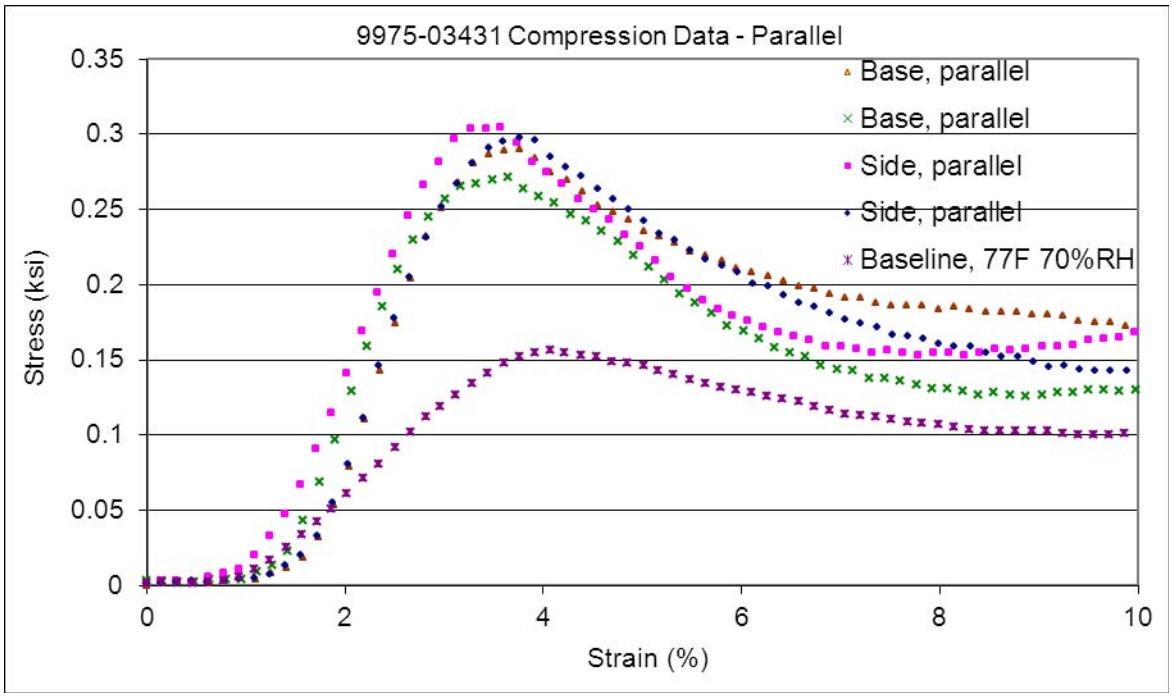

(b)

Figure 6. Fiberboard compression test data, compared with typical baseline (77°F, 70% RH) data, in the parallel orientation (i.e. load applied parallel to the fiberboard layers). The full curves are shown in (a), while the initial buckling region is expanded in (b).

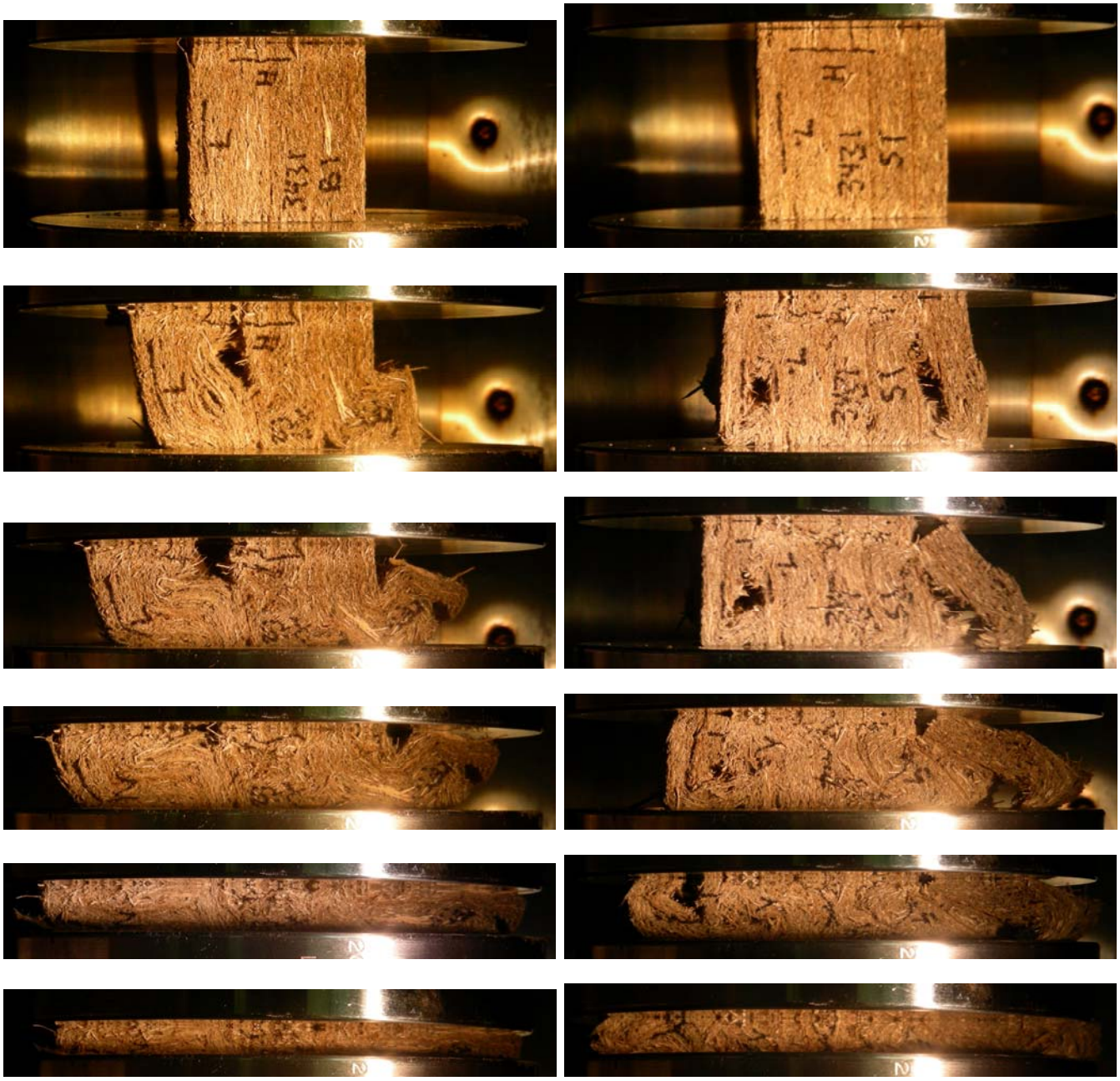

(a) Sample B1 from base of subassembly (b) Sample S1 from side of subassembly

Figure 7. Photographs of fiberboard samples during compression testing, parallel orientation

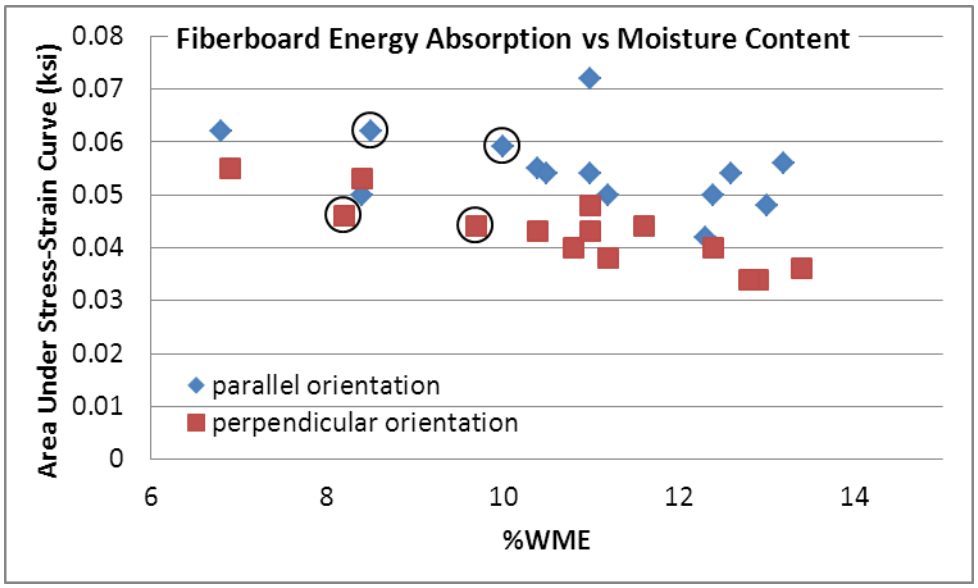

Figure 8. Fiberboard energy absorption, represented by the area under the stress-strain curve up to 40% strain, from tensile test samples from each destructively examined package. The results from 9975-03431 are circled.

Figure 9. Lead shield with corrosion product.

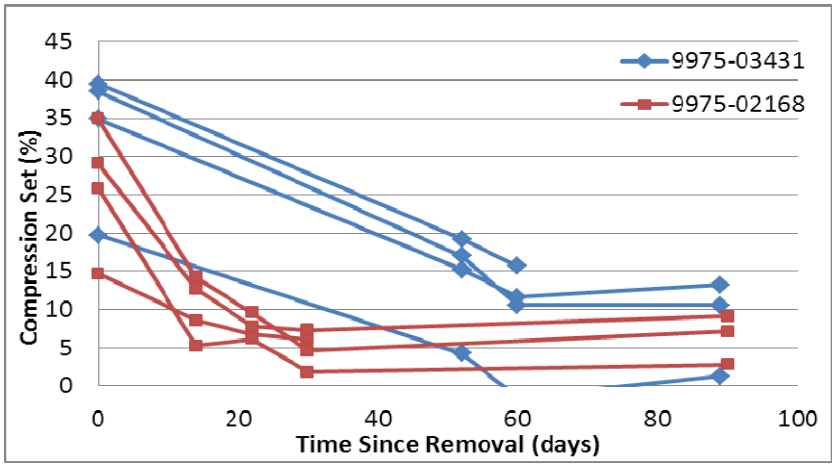

Figure 10. O-ring relaxation as indicated by change in compression set following removal during field surveillance. Results are shown for each of the 4 O-rings from 9975-03431, compared to similar data from 9975-02168.

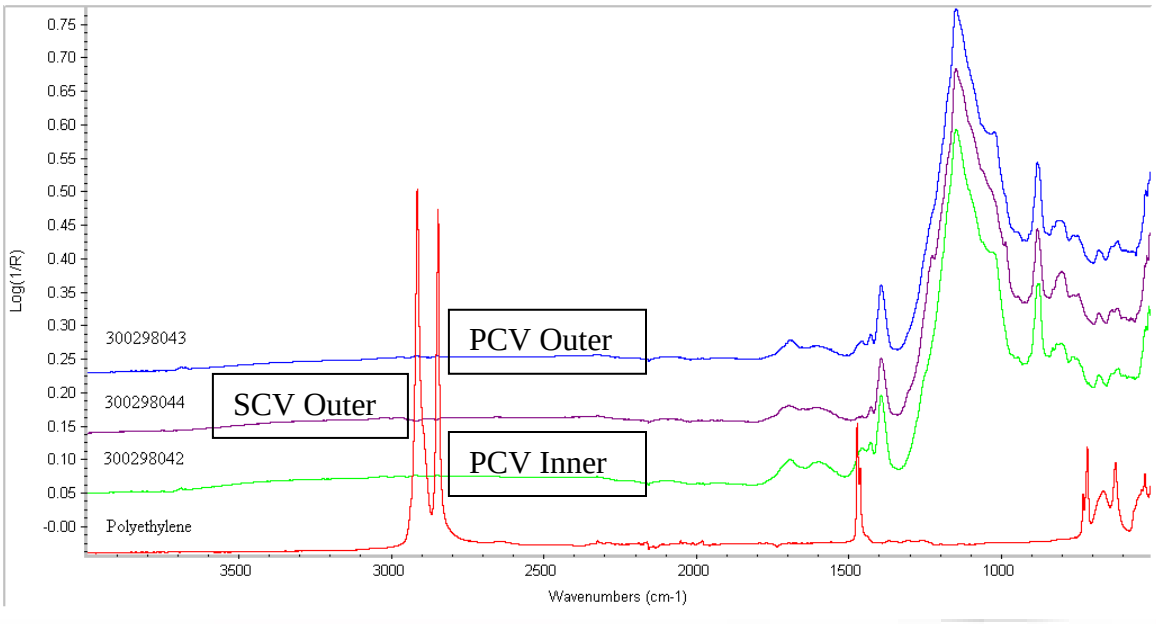

(a)

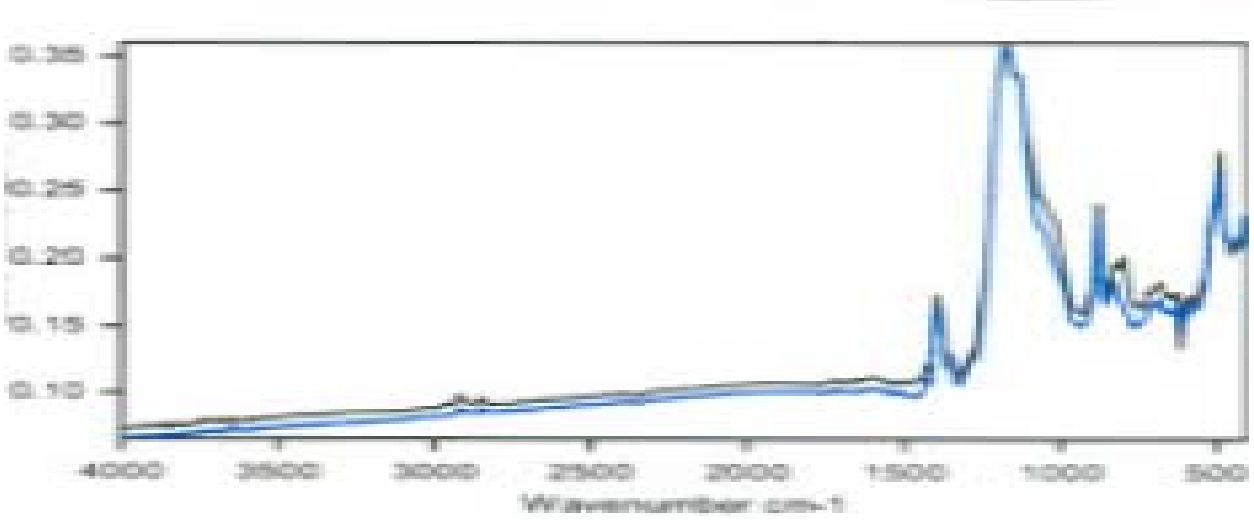

(b)

Figure 11. FT-IR spectra for the three tested O-rings (a). Each spectrum is consistent with a Viton® type fluoroelastomer (b).

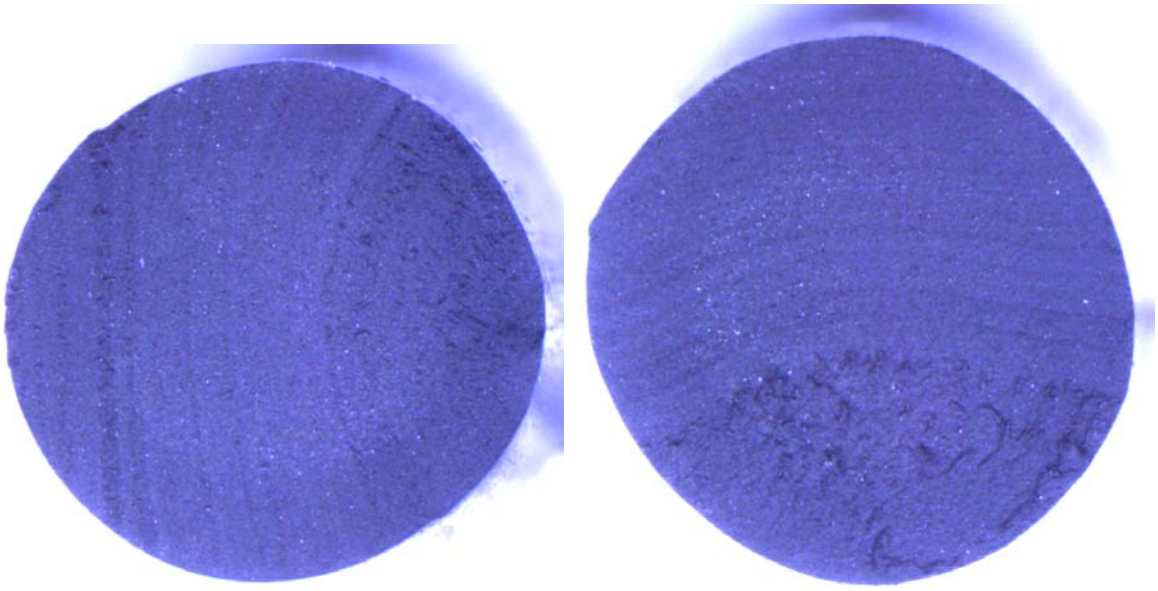

(a) (b)

Figure 12. Optical cross section of the (a) PCV outer and (b) SCV outer O-rings.

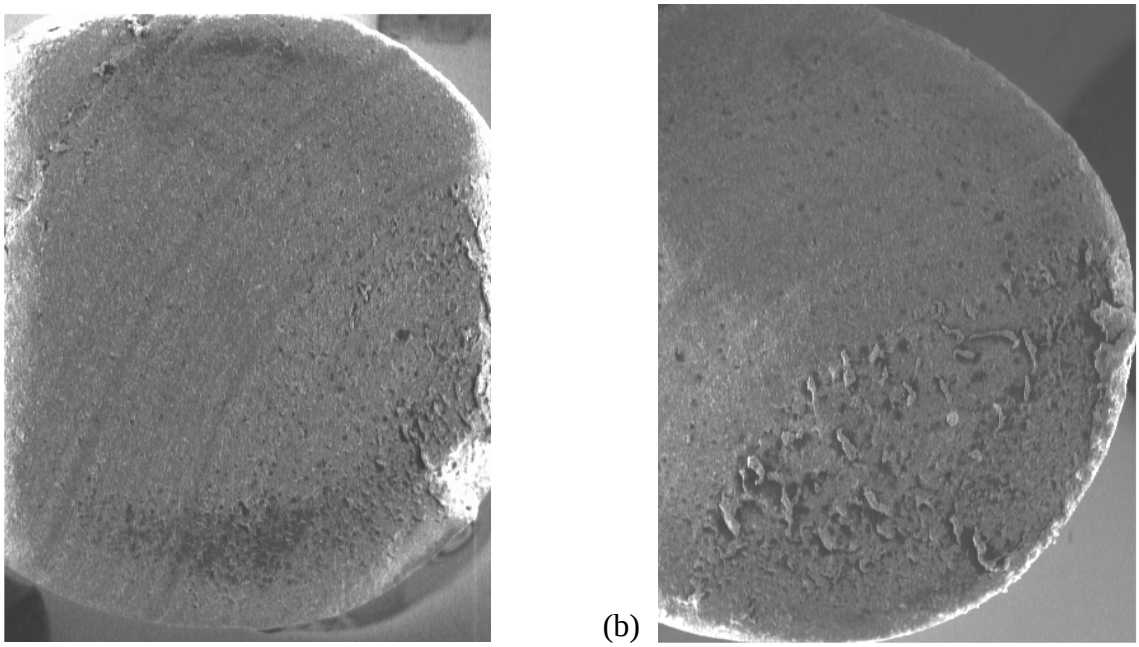

(a) (b)

Figure 13. SEM cross section of the (a) PCV outer and (b) SCV outer O-rings.

Figure 14. PCV inner O-ring during tensile test, at 50% stretch.

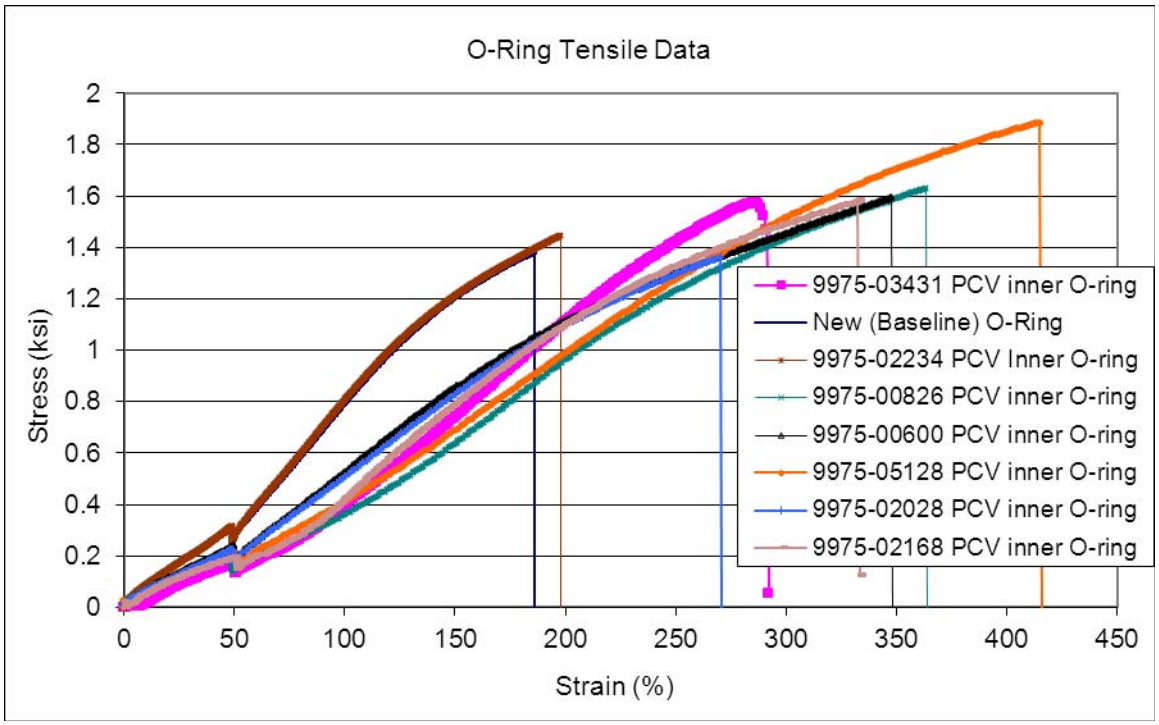

Figure 15. Tensile data for PCV inner O-ring from 9975-03431, compared to a new O-ring and the PCV O-rings from previously examined packages.

Attachment 1 9975-02028 Field Surveillance Results, with Comparison to Destructive Examination Results

Section I

Drum Exterior Examination

Item	Field Surveillance Result	Destructive Exam. Result
Drum vent plugs are specified and are in place as required	SAT	SAT
Drum surface is not dented beyond 0.25 inch	SAT	SAT
Drum Dents adjacent to the air shield are not deeper than 0.125 inch	SAT	SAT
Drum surface is free from corrosion, swelling/bulging and other physical damage	SAT	SAT

Comment – n/a

Section II

Humidity Measurements

Humidity at top of the drum 32.1 %RH

Section III

Temperature Measurements

[These data not repeated in this report.]

Section IV

Celotex® Inspection

Upper Celotex® Assembly Weight: 28.3 lb (field surv.) 12.865 kg / 28.36 lb (destructive exam)

Visual:

Item	Field Surveillance Result	Destructive Exam. Result
Inspect all exposed Celotex® surfaces for significant damage and ensure layers are well bonded	SAT	SAT
Upper Celotex® came out smoothly, without interference	SAT	SAT
All visible Celotex® surfaces are free from staining and variation in coloration	SAT	SAT
Celotex® is free from significant swelling (e.g. gap exists against drum), shrinkage and other significant physical damage	SAT	SAT
Lead shield is free from significant deformation and physical damage and shows no sign of flaking, blistering or spalling	SAT	SAT
Lead shield Go/No Go gauge went smoothly into the lead shield and reached all the way to the bottom of the lead shield	SAT	NA

Comments: n/a

Attachment 1 9975-02028 Field Surveillance Results, with Comparison to Destructive Examination Results

Celotex® Dimensions (all results reported in inches)

Dimensions		0°	90°	180°	270°	Field Surveillance Average	Destructive Exam. Average
1	Upper Assembly OD	17.674	17.675			17.674	17.684
2	Upper Assembly lower step OD	14.676	14.670			14.673	14.650
3	Upper Assembly ID	8.520	8.533			8.526	8.548
4	Upper Assembly inside height	5.024	5.025	5.028	5.035	5.028	5.034
5	Lower Assembly step height	2.063	2.077	2.051	2.060	2.063	2.062
6	Lower Assembly height from lower step to top of lead shield	4.220	4.216	4.215	4.211	4.216	NA

Dimension	Result	Criteria	Field Surveillance Result	Destructive Exam. Result
Dimension #6 average	4.216	$\leq$ 4.65"	SAT	NA
Dimension #1 average – Dimension #3 average	9.148	$\geq$ 8 3/16"	SAT	SAT

Section V

O-Ring Inspection

Test	SAT/UNSAT
O-ring seal test performed on SCV	SAT
SCV O-rings were removed intact	SAT
SCV O-rings have no excess accumulation of grease	SAT
O-ring seal test performed on PCV	SAT
PCV O-rings were removed intact	SAT
PCV O-rings have no excess accumulation of grease	SAT

Comments: n/a

Attachment 1 9975-02028 Field Surveillance Results, with Comparison to Destructive Examination Results

(all dimensional results reported in inches)

Action	0°	90°	180°	270°	Time	Destructive Exam. Average Result
Loosen SCV lid					1435	NA
Outer SCV O-Ring						
Measure OD (while on plug)	(5.285)*	(5.283)*			1448/1449	NA
Measure radial thickness	0.1265	0.1285	0.1360	0.1340	1449/1450	0.1396
Measure vertical thickness	01245				1450	0.1331
Inner SCV O-Ring						
Measure OD (while on plug)	(5.179)*	(5.178)*			1451/1452	NA
Measure radial thickness	0.1230	0.1245	0.1235	0.1240	1453/1453	NA
Measure vertical thickness	0.1345				1454	NA
Loosen PCV lid					1508	NA
Outer PCV O-Ring						
Measure OD (while on plug)	5.245	5.240			1512/1514	NA
Measure radial thickness	0.1260	0.1255	0.1250	0.1245	1515/1515	0.1344
Measure vertical thickness	0.1350				1516	0.1364
Inner PCV O-Ring						
Measure OD (while on plug)	5.129	5.130			1517/1518	NA
Measure radial thickness	0.1225	0.1240	0.1235	0.1235	1518/1519	NA
Measure vertical thickness	0.1335				1519	NA

* These dimensions (SCV O-Ring OD while on plug) are typically ~6.3 and ~6.2 inches. It is assumed that the recorded initial digit is a typographical error.

Attachment 1 9975-02028 Field Surveillance Results, with Comparison to Destructive Examination Results

SRNL Receipt Examination of O-Rings

VISUAL EXAMINATION

PCV	PCV Outer	PCV Inner
Grease present	yes	yes
Color (normal or explain)	Normal	Normal
Cross-sectional shape	round	round
Nicks, Scratches, Cracks	none	none
Other Damage (Note extent/size)	none	none
Picture (Note if taken)		

SCV	SCV Outer	SCV Inner
Grease (type, amount)	yes	yes
Color (normal or explain)	Normal	Normal
Cross-sectional shape	round	round
Nicks, Scratches, Cracks	none	none
Other Damage (Note extent/size)	none	none
Picture (Note if taken)		

THICKNESS (all results reported in inches)

PCV	PCV Outer		PCV Inner	
	Axial	Radial	Axial	Radial
Thickness 1 (in)	0.1360	0.1345	0.1355	0.1325
Thickness 2 (in)	0.1365	0.1313	0.1360	0.1305
Thickness 3 (in)	0.1370	0.1325	0.1370	0.1320
Thickness 4 (in)	0.1360	0.1335	0.1365	0.1305
Field Surv. Average	**0.1364**	**0.1330**	**0.1362**	**0.1314**
Destructive Exam Average	**0.1364**	**0.1344**		

SCV	SCV Outer		SCV Inner	
	Axial	Radial	Axial	Radial
Thickness 1 (in)	0.1335	0.1395	0.1370	0.1330
Thickness 2 (in)	0.1340	0.1365	0.1350	0.1315
Thickness 3 (in)	0.1325	0.1360	0.1350	0.1315
Thickness 4 (in)	0.1325	0.1370	0.1365	0.1330
Field Surv. Average	**0.1331**	**0.1373**	**0.1359**	**0.1323**
Destructive Exam Average	**0.1331**	**0.1396**		

Attachment 1 9975-02028 Field Surveillance Results, with Comparison to Destructive Examination Results

SRNL Receipt Examination of O-Rings (Continued)

HARDNESS

	PCV O-Rings		SCV O-Rings	
	Outer	Inner	Outer	Inner
Hardness 1, M-Scale	80.0	80.0	79.0	7930
Hardness 2, M-Scale	80.0	80.0	79.0	78.0
Hardness 3, M-Scale	79.0	80.5	78.5	78.0
Hardness 4, M-Scale	79.5	80.5	79.0	78.5
Hardness 5, M-Scale	79.5	80.0	79.0	78.5
Average	**79.5**	**80.2**	**78.9**	**78.4**

CONTINUATION:
NA

CC: T. M. Adams, 773-41A
J. S. Bellamy, 730-A
G. T. Chandler, 773-A
W. L. Daugherty, 773-A
K. A. Dunn, 773-41A
T. J. Grim, 105-K
E. R. Hackney, 705-K
D. R. Leduc, 730-A
J. W. McClard, 705-K
J. W. McEvoy, 707-42B
J. L. Murphy, 730-A
T. E. Skidmore, 730-A
Document Control